



Comparing the effects of chlorination on membrane integrity and toxin fate of high- and low-viability cyanobacteria

Xi Li ^{a, b}, Sheng Chen ^{a, b}, Jie Zeng ^{a, b}, Weijun Song ^d, Xin Yu ^{a, c, *}

^a Key Lab of Urban Environment and Health, Institute of Urban Environment, Chinese Academy of Sciences, Xiamen, 361021, China

^b University of Chinese Academy of Sciences, Beijing, 100049, China

^c College of The Environment & Ecology, Xiamen University, Xiamen, 361102, China

^d College of Ecological and Resources Engineering, Wuyi University, Wuyishan, 354300, China

ARTICLE INFO

Article history:

Received 30 November 2019

Received in revised form

27 March 2020

Accepted 28 March 2020

Available online 2 April 2020

Keywords:

Chlorine

Cyanobacteria

Cell viability

Membrane integrity

Toxin fate

ABSTRACT

Occurrence of toxic cyanobacterial blooms in natural freshwaters could impair drinking water quality. Chlorine was often employed as an oxidant to treat algal-laden source waters in drinking water treatment plants. However, previous studies only focused on high-viability cyanobacteria at exponential phase. Whether the change of cell-viability of cyanobacteria could affect chlorination was unknown. Here, high- and low-viability *Microcystis* were collected from a whole life cycle of cyanobacteria in lab-scale, and effects of chlorination on membrane integrity and toxin fate of high- and low-viability *Microcystis* were subsequently investigated. Results showed chlorine exposure was lower for low-viability cells than high-viability cells with the same initial chlorine dosage, but low-viability cells were less resistant to chlorination, leading to higher rate of membrane damage (k_{loss}) and intracellular toxin release (k_i). For high-viability cells, there was no increase of extracellular toxin with sufficient chlorine exposure whereas it showed a continuous increase for low-viability cells mainly due to its lower rate of extracellular toxin degradation (k_e , $26 \pm 8 \text{ M}^{-1} \text{ s}^{-1}$) than intracellular toxin release (k_i , $110 \pm 16 \text{ M}^{-1} \text{ s}^{-1}$) ($k_e < k_i$). Besides, total toxin could be completely oxidized for high-viability cells with sufficient chlorine exposure ($>30 \text{ mg min L}^{-1}$) whereas chlorination could not work well for low-viability cells even with chlorine exposure of as high as 36 mg min L^{-1} . These findings indicated chlorination may not be a feasible option to treat low-viability cyanobacteria during decline stage of cyanobacterial blooms.

© 2020 Published by Elsevier Ltd.

1. Introduction

Cyanobacterial blooms in eutrophication lakes and reservoirs have increasingly become a major environmental concern worldwide. Cyanobacterial cells and related metabolites (e.g., cyanotoxins) have posed serious threats to drinking water safety and challenged drinking water treatment plants (DWTPs) (Zamyadi et al., 2012a; He et al., 2016). *Microcystis* species are one of the most common and problematic species and produce a range of microcystins (MCs) (Harke et al., 2016). To date, more than 100 variants of MCs (e.g., MC-LR, MC-YR, MC-RR) were reported. Among these MCs, MC-LR is the most common microcystin and has been

proven to be potent liver tumor promoter, posing a high risk of human health (Falconer et al., 1983; Sivonen and Jones, 1999; Pearson et al., 2010). Hence, World Health Organization has established a guideline safety value of $1 \mu\text{g L}^{-1}$ (MC-LR) in drinking water (WHO, 2014). Besides, the presence of cyanobacteria can also cause process disturbances in DWTPs using filtration, such as excessive head loss development, shorter filter runs and higher coagulant demands (Mouchet and Bonnelye, 1998; Merel et al., 2010).

Chlorine, as the most common disinfectant in DWTPs, is also employed as an oxidant to treat algal-laden source waters. Direct chlorination of source water, inter- or post-chlorination is widely applied in DWTPs in many developing countries (e.g., China and India) and North America. Chlorination could inactivate cyanobacteria via destroying cellular contents, leading to cytolysis, corrosion and wrinkling of cell wall and cytoplasmic membrane (Ou et al., 2011). Besides, prior to coagulation, chlorination could

* Corresponding author. Key Lab of Urban Environment and Health, Institute of Urban Environment, Chinese Academy of Sciences, Xiamen, 361021, China.

E-mail addresses: xyu@iue.ac.cn, xyu@xmu.edu.cn (X. Yu).

improve removal efficiency of cyanobacteria by altering cell surface properties to enhance solid-liquid separation (Plummer and Edzwald, 2002). Furthermore, chlorination is highly efficient for the oxidation of cyanotoxins under various water quality conditions (Nicholson et al., 1994; Acero et al., 2005; Ho et al., 2006; Rodriguez et al., 2007; Merel et al., 2010; Zamyadi et al., 2010, 2012b; 2013; Fan et al., 2014, 2016). Therefore, chlorination is a feasible option to prevent the breakthrough of cyanobacteria and toxin into drinking water.

However, some studies reported algal organic matters (AOMs) could be precursors of disinfection by-products (DBPs) after chlorination (Zamyadi et al., 2012b, 2013). What's worse, chlorination could induce membrane damage, leading to the release of intracellular toxin (Daly et al., 2007; Zamyadi et al., 2012b; Fan et al., 2013, 2014). To address this issue, many studies have investigated the kinetics of cell lysis and toxin fate after chlorination, and found the susceptibility of cyanobacteria to chlorination is influenced by species, morphology, cell counts and oxidative conditions (e.g., temperature, pH, dosages, contact time, water matrix) (Daly et al., 2007; Lin et al., 2009; Zamyadi et al., 2012b). For example, Lin et al. (2009) reported cell lysis rate of *Anabaena circianlis* ($1400\text{--}3400\text{ M}^{-1}\text{ s}^{-1}$) was higher than *Microcystis aeruginosa* ($790\text{--}1100\text{ M}^{-1}\text{ s}^{-1}$), and Fan et al. (2016) found colonial *Microcystis* were more resistant to chlorination than unicellular cells due to the protection of mucilaginous surrounding cells. Meanwhile, Zamyadi et al. (2013) and Fan et al. (2014) demonstrated there was no increase of extracellular toxin after chlorination, since the rate of extracellular toxin oxidation was faster than the rate of intracellular toxin release. However, the majority of these data were gained from chlorination experiments conducted using high-viability cyanobacteria at exponential phase.

Actually, in natural freshwaters, historical observations showed cyanobacterial bloom was a successive process lasting for several months in a year, including development, maintenance and decay stage (Guo, 2007; Tang et al., 2018). During maintenance and decay stage, Tang et al. (2018) found the genes of N and P metabolism were down-regulated via meta-transcriptome analysis of bloom samples from Taihu lake (China), indicating nutrition limitation may induce a decrease of cell-viability at this stage. For low-viability cyanobacteria at maintenance and decay stages, Tang et al. (2018) also found *mcyE* gene was up-regulated, suggesting toxin would accumulate in these low-viability cyanobacteria. Besides, Rivasseau et al. (1998) and Pietsch et al. (2002) observed an increase of extracellular toxin in pure-culture cyanobacteria at stationary phase, and Ziegmann et al. (2010) also observed the highest ratio of MC-LR/Chl a of *M. aeruginosa* at decline phase. These results indicated low-viability cells would pose a higher toxin risk than high-viability cells. The difference of chlorination in treating high- and low-viability cyanobacteria is not clear, and whether chlorination is a feasible option to treat low-viability cyanobacteria and control toxin risk is also unknown. Thus, it is of great importance to compare the chlorination process to treat high- and low-viability cyanobacteria.

To date, no studies have investigated the impact of chlorination on low-viability cyanobacteria and related metabolites. In this study, a whole life cycle of *Microcystis* in lab-scale was established to collect high- and low-viability cells to conduct chlorination experiments. The effects of chlorination on membrane integrity loss and toxin release and degradation of high- and low-viability *Microcystis* were investigated and compared, aiming to discuss the appropriateness of chlorination to treat low-viability cyanobacteria at decline stage of a successive bloom.

2. Materials and methods

2.1. Materials and reagents

A toxic strain *Microcystis aeruginosa* FACHB-915 was purchased from the Institute of Hydrobiology, Chinese Academy of Sciences. It was cultured in BG11 medium at 28 °C under constant light flux ($35\text{ }\mu\text{mol of photons m}^{-2}\text{ s}^{-1}$) with a 12 h:12 h light-dark cycle in an incubation cabinet equipped with cold light source Light Emitting Diode (LED) (GXZ-280C; China).

Sodium hypochlorite commercial solutions for chlorination experiments were analytical grade (Sigma, German). SYTOX Green nucleic acid stain for membrane integrity analysis was purchased from Thermo Fisher Scientific (USA). MC-LR standards, methanol and monobasic potassium phosphate for toxin analysis were chromatographically grade and purchased from Solarbio (China). Moreover, all solutions were prepared using ultra-pure water purified to a resistivity of 18 M Ω cm by a Milli-Q water purification system (Millipore Pty Ltd, USA).

2.2. Samples preparation of high- and low-viability microcystis

A whole life cycle of *Microcystis* in lab-scale was established. In BG-11 medium, *Microcystis* growth was monitored for 100 d, and cell counts were quantified at each five days during cultivation. Samples for cell counts were treated with Lugol's iodine, and counted with blood counting chamber (Qiuqing, China) by microscopy (OLYMPUS BX43, Japan) at 400 \times magnification. The growth pattern of *Microcystis* mainly includes three classical growth phases: exponential (5–30 d), stationary (30–70 d) and decline growth phase (70–100 d) (Fig. 1).

Microcystis samples of 10 mL at exponential (15 d), stationary phase (50 d) and decline phase (90 d) were centrifuged at 6000 g for 5 min, and cells were collected and washed with double-distilled water (ddH₂O) twice. Cell morphology of *Microcystis* at all three phases were observed using electron microscope techniques, as described below. Moreover, photosynthetic yield (ϕ_{PSII}) is an indicator of the photosynthetic performance of phytoplankton and widely used as a sensitive indicator of cell viability. Hence, ϕ_{PSII} of *Microcystis* was also measured, respectively, and the method was described in details below.

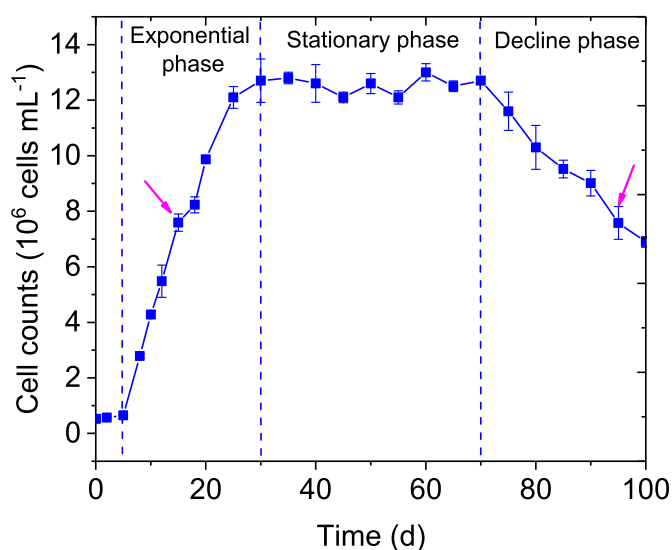


Fig. 1. Growth curve of *Microcystis* from 0 to 100 d in BG-11 medium.

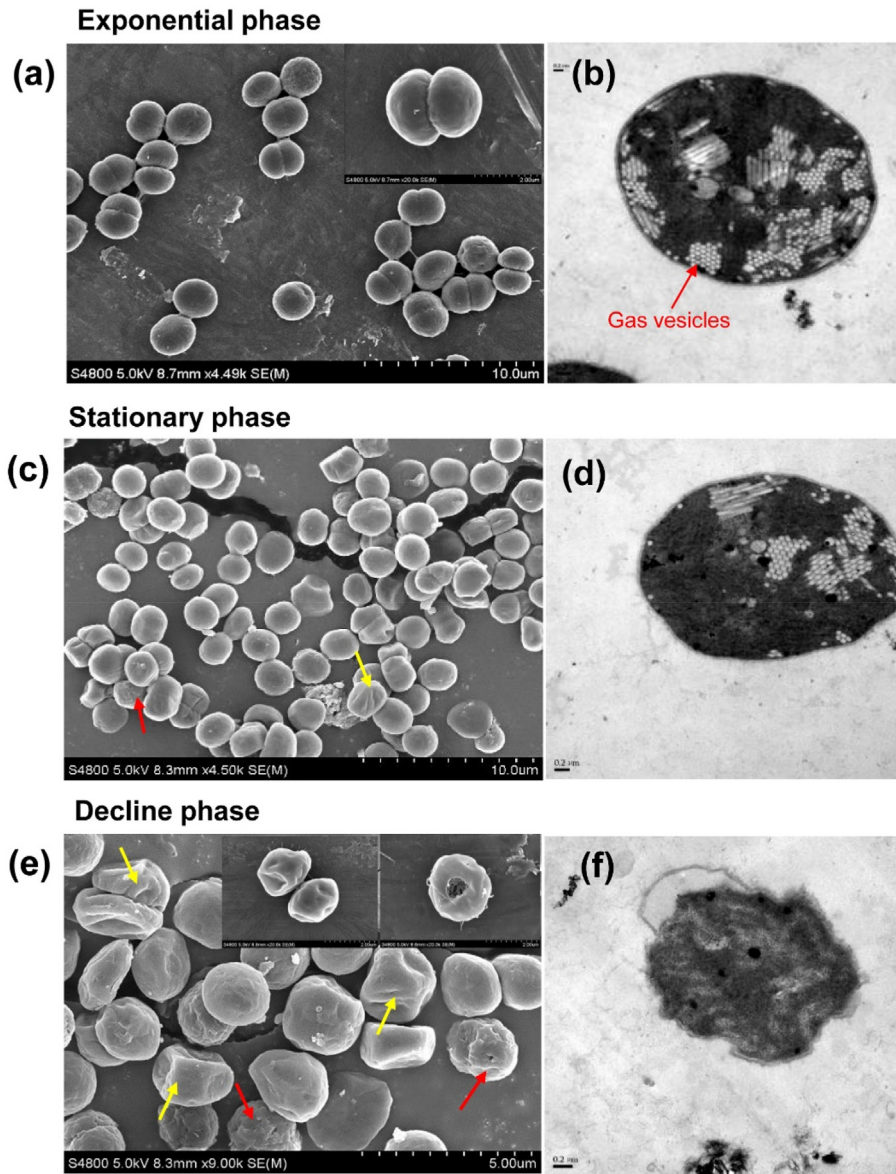


Fig. 2. Morphology characteristics of *Microcystis* at exponential (15 d), stationary (50 d) and decline phase (90 d) observed by SEM and TEM. SEM images of cell surface at exponential (a), stationary (c) and phase (e). TEM images of cell ultrathin slices at exponential (b), stationary (d) and decline phase (f).

For *Microcystis* at exponential phase, intact intracellular structures comprising of nucleus area, photosynthetic lamella and gas vesicles were clearly observed in cells (Fig. 2b). Most of these cells appeared in pairs (Fig. 2a), and cell counts kept increasing with high ϕ_{PSII} of 0.37, suggesting these cells were reproducing via cell division and maintained high-viability. After 30 d cultivation, *Microcystis* in pairs disappeared and intracellular gas vesicles became reduced (Fig. 2c and d), but cell-density remained at the maximum of about 1.2×10^7 cells mL^{-1} for 40 d and ϕ_{PSII} of *Microcystis* did not show significant difference between cells at stationary phase and exponential phase ($P > 0.05$) (Figs. 1; 3). These results suggested the majority of *Microcystis* at stationary stage remained high-viability, as the same as *Microcystis* at exponential phase. In contrast, for *Microcystis* at decline phase, cell-density strikingly declined and ϕ_{PSII} of *Microcystis* (0.21) was significantly lower than cells at exponential and stationary phase (0.36–0.37) ($P < 0.05$) (Figs. 1; 3). Besides, *Microcystis* cells became shrinking (yellow arrows) or irregular shaped, and several cells became

severely damaged (red arrows) with holes on cell surfaces (Fig. 2e). Intracellular structures in some cells were destroyed to some extent as well (Fig. 2f; 2e). These results indicated cell-viability of *Microcystis* strikingly declined at this stage. To achieve the same initial cell-density of high- and low-viability cells, *Microcystis* were collected at exponential (15 d) and decline phase (90 d) to conduct chlorination experiments, and these samples could well represent high- and low-viability of *Microcystis*, respectively (Fig. 1, red arrows).

2.3. Chlorination experiments

International Joint Commission and Ohio Environmental Protection Agency (EPA) have set a chlorophyll *a* threshold of $50 \mu\text{g L}^{-1}$ for severe blooms, and corresponding cell density was greater than 1×10^5 cells mL^{-1} (Watson and Boyer, 2013; Kasich et al., 2014). Besides, previous studies have performed extensive chlorination experiments for high-viability *Microcystis* of 10^5 – 10^6 cells mL^{-1}

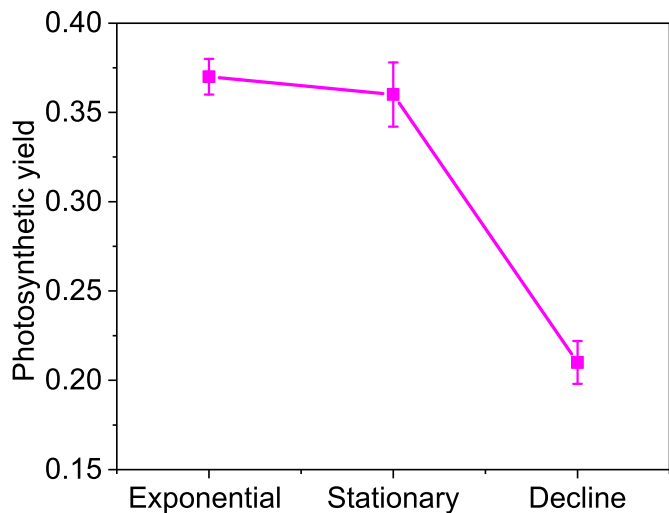


Fig. 3. Photosynthetic yield (ϕ_{PSII}) of *Microcystis* at exponential (15 d), stationary (50 d) and decline phase (90 d).

(Daly et al., 2007; Zamyadi et al., 2012b, 2013; Fan et al., 2013, 2014; Qi et al., 2016). Therefore, prior to chlorination experiments, initial cell-density (7.6×10^6 cells mL⁻¹) of high- and low-viability *Microcystis* samples were equally diluted with ddH₂O to achieve a final cell density of 1×10^6 cells mL⁻¹. In addition, toxin degradation was highly dependent on pH and could be significantly reduced above 8 (Nicholson et al., 1994). Hence, cultures were adjusted to pH 7.5 ± 0.1 before chlorination experiments using 0.1 M sodium hydroxide or hydrochloric acid (Daly et al., 2007; Fan et al., 2013, 2014).

A chlorine stock solution was prepared by sodium hypochlorite commercial solutions. Free chlorine concentration was measured using the N, N, diethyl-pphenylenediamine (DPD) method (APHA et al., 1998). For chlorination experiments, *Microcystis* samples were treated with the desired concentrations (1, 2, 4 and 8 mg L⁻¹), according to the applied dosages for high-viability *Microcystis* at exponential phases in previous studies (Daly et al., 2007; Zamyadi et al., 2012b, 2013; Fan et al., 2013, 2014; 2016; He and Wert, 2016; Qi et al., 2016). All chlorination experiments with 2 L reaction suspension were conducted in 5 L glass conical flasks and incubated in darkness at room temperature (20 ± 2 °C). During chlorination, *Microcystis* samples were taken at specified contact time (0, 1, 2, 4, 8, 16, 32 and 60 min), and immediately analyzed to determine the chlorine residual using the DPD-FAS titration methods (APHA et al., 1998). At each time interval, samples with specific volumes were quenched with sodium thiosulfate at a stoichiometric ratio specified in Standard Methods (APHA et al., 1998), and prepared for the following analysis of membrane integrity and toxin. Besides, *Microcystis* samples without adding chlorine were conducted as control tests.

2.4. Analytical methods

2.4.1. Electron microscopes observation

Microcystis samples of 10 mL were collected at exponential (15 d), stationary (50 d) and decline phase (90 d), centrifuged by 6000 g for 5 min and washed with phosphate buffer saline twice (PBS 10 mM, pH 7). Cellular surface structures of *Microcystis* were observed using a scanning electron microscope (SEM) (Hitachi S-4800, Japan), according to Li et al. (2019). Besides, intracellular structures were further observed using a transmission electron microscope (TEM) (Hitachi H-7650, Japan), and the details were described in supplementary material Text S1.

2.4.2. Photosynthetic capacity quantification

Microcystis samples of 10 mL were collected at exponential (15 d), stationary (50 d) and decline phase (90 d), centrifuged by 6000 g for 5 min, washed with phosphate buffer saline twice (PBS 10 mM, pH 7), and then diluted with ddH₂O to achieve the same cell density of 1×10^5 cells mL⁻¹. Prior to analysis, samples of 5 mL were treated in darkness for 10 min, after which photosynthetic yield was measured using PHYTO-PAM phytoplankton analyzer (Walz, Germany). Photosynthetic yield (ϕ_{PSII} , also known as quantum yield of PSII electron transport) can be calculated according to Maxwell and Johnson (2000):

$$\phi_{PSII} = (F_m - F_0) / F_m \quad (1)$$

where F_0 and F_m are the minimum and maximum fluorescence, respectively. After saturating flashes are applied, a value for F_m was the maximum fluorescence in this light, and steady-state value of fluorescence immediately prior to the flash is termed as minimum fluorescence of F_0 (Maxwell and Johnson, 2000).

2.4.3. Membrane integrity determination

During chlorination, *Microcystis* samples of 1 mL were taken at specified contact time (0, 1, 2, 4, 8, 16, 32 and 60 min), and immediately quenched with sodium thiosulfate. At each time interval, membrane integrity was determined using a visual flow cytometry (FCM) (Flowsight, Meck milipore, USA). If cellular membrane was destroyed, SYTOX Green nucleic acid stain could permeate into cells and bind to DNA, resulting in bright green fluorescence with emitting a fixed wavelength of 488 nm. Thus, the stain was used to determine damaged cells after chlorination (SYTOX positive, green fluorescence), as described by Daly et al. (2007). In contrast, there was only red fluorescence for intact cells, since SYTOX Green could not permeate into cells and pigments themselves showed red fluorescence with emitting a fixed wavelength of 488 nm using FCM (SYTOX negative, red fluorescence). Each sample (200 μ L) was incubated for 10 min after adding SYTOX Green nucleic acid stain with a final concentration of 1 μ M, and run for approximately 2–5 min. Approximately 10000 events (cells) were recorded by the flow cytometry, and percentage of intact cells was analyzed using flow cytometric analysis software (Flowsight, Meck Millipore, USA).

2.4.4. Microcystin quantification

During chlorination, *Microcystis* samples of 100 mL were taken at specified contact time (0, 1, 2, 4, 8, 16, 32 and 60 min), and immediately quenched with sodium thiosulfate. At each time interval, 50 mL were centrifuged by 6000 g for 5 min to collect cells for intracellular toxin measurement, and the remaining (50 mL) was for total toxin measurement (Fan et al., 2014). Prior to toxin analysis, extracted toxin from samples was concentrated by C18 solid-phase extraction with supelcleanTM ENVITM-18 SPE tubes (USA) (Nicholson et al., 1994). In this study, *M. aeruginosa* FACHB-915 only produce MC-LR in our culture (Fig. S1), and thus, concentration of MC-LR was measured by a high-performance liquid chromatography (HPLC) (Agilent 1200, USA) using UV 238 nm with a flow rate of 1 mL min⁻¹ on a Bio-C18 column (Sepax, USA, 4.6 \times 250 mm, 5 μ m) at 25 °C. Mobile phase was consisted of methanol (phase A) and 0.05 M monobasic potassium phosphate (KH₂PO₄, pH 3) (phase B) with volume ratio of 57: 53.

2.4.5. Dissolved organic carbon characterization

Prior to chlorination, high- and low-viability *Microcystis* samples of 1×10^6 cells mL⁻¹ with a volume of 10 mL were taken and filtrated with 0.45 μ m Millipore Express[®] PVDF filter (German) to remove cells. This filter could not absorb organic matters and thus, it did not affect subsequent DOC analysis (Fig. S2). Dissolved

organic carbon (DOC) concentration was measured by persulfate wet oxidation technique (Shimadzu TOC-V WP, Japan). Besides, UV absorbance at 254 nm (UV_{254}) of these samples was measured using a UV3600 Spectrophotometer (Shimadzu, Japan) with the optical path of 1 cm, and specific UV absorbance at 254 nm (SUVA) was calculated via following equation (2).

$$SUVA(\text{Lmg}^{-1} \text{ m}^{-1}) = UV_{254}(\text{cm}^{-1}) \times 100 / \text{DOC}(\text{mg L}^{-1}) \quad (2)$$

2.5. Statistics analysis

All experiments were conducted in triplicate, and error bars in the plots represented the standard deviation (SD) values. All data were statistically analyzed using Student's t-test, and differences were considered significant at $P < 0.05$.

3. Results

3.1. Chlorine decay

Chlorine of 1–8 mg L^{-1} was employed to treat high- and low-viability *Microcystis*, and there was a significant difference in chlorine consumption between high- and low-viability *Microcystis* (Fig. 4). For low-viability cells, there was no chlorine residual detected in treatments of 1, 2, 4 mg L^{-1} after 8, 16, 60 min, while residual concentrations of 0.3, 0.8 and 0.5 mg L^{-1} were detected for high-viability cells, respectively (Fig. 4). Besides, with initial highest dosage of 8 mg L^{-1} , a chlorine residual of 0.6 mg L^{-1} for low-viability cells was much lower than that for high-viability cells after a contact time of 60 min (residual chlorine of 3.5 mg L^{-1}) (Fig. 4).

During chlorination, chlorine decay showed the same fast-slow pattern in all treatments. To compare chlorine decay between high- and low-viability cells, fast-slow process of chlorine decay were modeled as a parallel first-order reaction (Fig. 4), and rate constants of each process was given by k_{fast} and k_{slow} according to Equation (3), as described by Daly et al. (2007).

$$Cl(t) = Cl_{fast}e^{-k_{fast}t} + Cl_{slow}e^{-k_{slow}t} + Cl_{v,slow} \quad (3)$$

where t = contact time; $Cl(t)$ = residual chlorine concentration at any time t ; Cl_{fast} = chlorine demand of fast reactions; Cl_{slow} = chlorine demand of slow reactions; k_{fast} = rate constant of

rapid reactions; k_{slow} = rate constant of slow reactions; $Cl_{v,slow}$ = amount of chlorine that was not reacted by fast or slow reactions.

Table 1 showed correlation coefficients (R^2) were determined to be 0.99–1.00 and Residual Sum of Squares (RSS) were much less than 0.05, suggesting the model fitted well (Table 1). With the same initial chlorine dosages, both k_{fast} and k_{slow} of low-viability cells were much higher than that of high-viability cells ($P < 0.05$), for example, k_{fast} of $0.73 \pm 0.02 \text{ min}^{-1}$ (RSS: 2.12×10^{-2}) was estimated for low-viability cells whereas lower value of $0.48 \pm 0.05 \text{ min}^{-1}$ (RSS: 1.48×10^{-2}) was for high-viability cells with chlorination of 8 mg L^{-1} (Table 1).

3.2. Membrane integrity loss

Prior to chlorination, about 90% of high-viability *Microcystis* remained intact and cellular surface was smooth, while over 50% were damaged for low-viability cells and damaged cellular membrane was observed in certain low-viability cells (Fig. 2; 5). Without chlorine exposure, percentage of intact cells of both low- and high-viability cells remained constant (Fig. 5). However, chlorination of 4–8 mg L^{-1} caused complete loss of membrane integrity of both low- and high-viability cells after 2–8 min contact time (Fig. 5). Even dosing with low chlorine dosages of 1–2 mg L^{-1} , more than 98% of intact cells were almost destroyed within 32–60 min (Fig. 5).

3.3. Membrane damage rate

To compare the impact of chlorination on membrane damage of high- and low-viability *Microcystis*, modified Chick/Watson model was employed to estimate membrane damage rate (k_{loss}) by fitting the number of intact cells over chlorine exposure (Fig. S3), as described by Daly et al. (2007). The equation was shown below (Equation (4)):

$$\ln\left(\frac{N_t}{N_0}\right) = -k_{loss}ct \quad (4)$$

Where ct = chlorine exposure; N_t = number of intact cells after a given chlorine exposure; N_0 = number of intact cells at $ct = 0$; and k_{loss} = rate constant of membrane damage.

Values of ct were calculated from chlorine decay data. Table 2 showed R^2 were between 0.94 and 1.00, and RSS (1.66×10^{-11} – 1.28×10^{-2}) were less than 0.05, suggesting the model fitted well. With the same initial dosages of chlorination, k_{loss} of low-viability

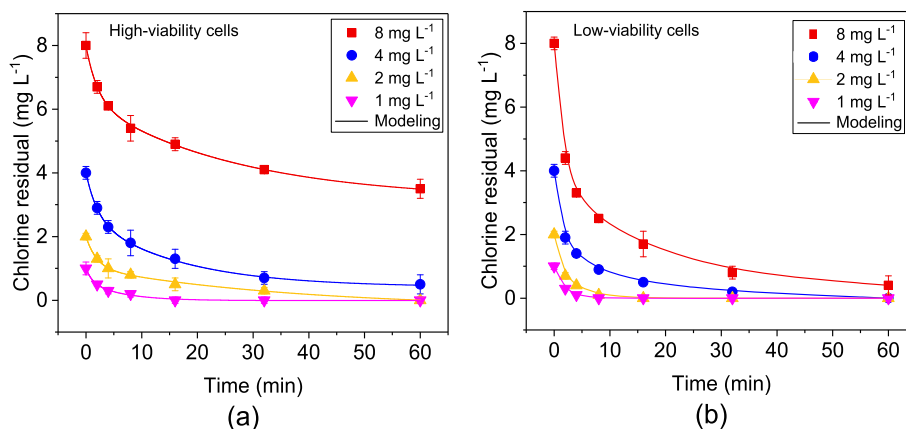


Fig. 4. Chlorine decay and fitted to a parallel first-order reaction model of high- (a) and low-viability *Microcystis* (b) treated with various doses of chlorine (1, 2, 4 and 8 mg L^{-1}) after a contact time of 60 min.

Table 1
Chlorine decay rates (k_{fast} , k_{slow}) of high- and low-viability *Microcystis* treated with various doses of chlorine (1, 2, 4 and 8 mg L⁻¹).

Dose (mg L ⁻¹)	High-viability cells						Low-viability cells					
	k_{fast} (min ⁻¹)	SE	k_{slow} (min ⁻¹)	SE	R ²	RSS	k_{fast} (min ⁻¹)	SE	k_{slow} (min ⁻¹)	SE	R ²	RSS
1	0.91 ^a	0.06	0.16 ^a	0.02	0.99	3.72×10^{-2}	2.24 ^a	0.14	0.55 ^a	0.03	1.00	9.53×10^{-5}
2	0.51	0.08	0.03	0.01	0.99	1.75×10^{-2}	4.56 ^a	0.02	0.29 ^a	0.04	0.99	5.02×10^{-4}
4	0.49	0.03	0.05	0.01	1.00	4.68×10^{-2}	0.83	0.15	0.08	0.02	0.99	6.69×10^{-3}
8	0.48	0.05	0.04	0.01	0.99	1.48×10^{-2}	0.73	0.02	0.06	0.002	1.00	2.12×10^{-2}

SE: standard errors of k_{fast} and k_{slow} . R²: correlation coefficients. RSS: residual sum of squares.

^a Values were not accurately estimated due to insufficient data.

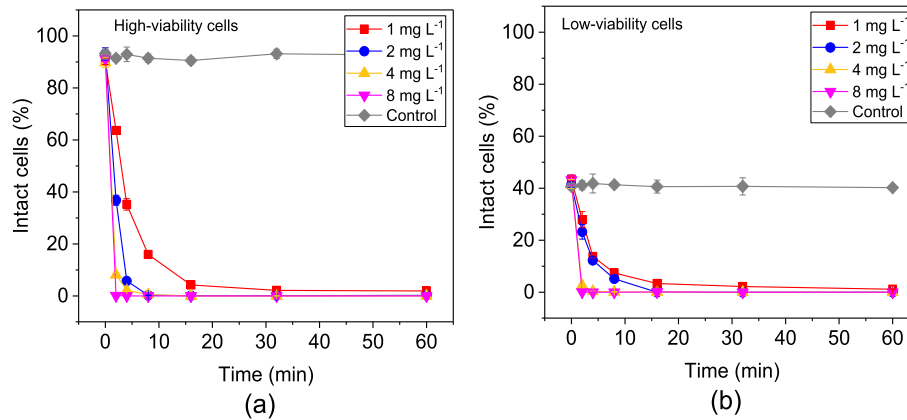


Fig. 5. Percentage of intact cells of high- (a) and low-viability *Microcystis* (b) treated with various doses of chlorine (1, 2, 4 and 8 mg L⁻¹) after a contact time of 0, 2, 4, 8, 16, 32 and 60 min.

Table 2
Membrane damage rate (k_{loss}) of high- and low-viability *Microcystis* treated with various doses of chlorine (1, 2, 4 and 8 mg L⁻¹).

Dose (mg L ⁻¹)	High-viability cells				Low-viability cells			
	k_{loss} (M ⁻¹ s ⁻¹)	SE	R ²	RSS	k_{loss} (M ⁻¹ s ⁻¹)	SE	R ²	RSS
1	726 ^a	32	0.95	1.28×10^{-2}	818 ^a	34	0.99	1.53×10^{-4}
2	410	19	0.97	4.90×10^{-3}	809 ^a	32	0.94	3.52×10^{-3}
4	361	2	0.99	1.05×10^{-5}	532	8	0.99	1.67×10^{-3}
8	445	3	1.00	1.66×10^{-11}	672	2	0.99	1.56×10^{-11}
Average	486 ± 164				708 ± 135			

SE: standard errors of k_{loss} . R²: correlation coefficients. RSS: residual sum of squares.

^a Values were not accurately estimated due to insufficient data.

cells was much higher than that of high-viability cells ($P < 0.05$) (Table 2). Besides, average k_{loss} ($708 \pm 135 \text{ M}^{-1} \text{ s}^{-1}$) of low-viability cells was also higher than that of high-viability cells ($486 \pm 164 \text{ M}^{-1} \text{ s}^{-1}$) ($P < 0.05$) (Table 2).

3.4. Total toxin degradation

Prior to chlorination, total toxin of low-viability cells ($170 \mu\text{g L}^{-1}$) was much higher than high-viability cells ($44 \mu\text{g L}^{-1}$) ($P < 0.05$), but chlorination could effectively oxidize toxin to some extent for both high- and low-viability cells (Fig. 6). For high-viability cells, about 6 and $25 \mu\text{g L}^{-1}$ of total toxin was present after 60 min with initial low chlorine of 2 and 1 mg L^{-1} , while total toxin was degraded to below detection limits after 32–60 min with high dosage of 4 and 8 mg L^{-1} (Fig. 6a). In contrast, total toxin of $68\text{--}168 \mu\text{g L}^{-1}$ was residual after 60 min with chlorination of 1–8 mg L⁻¹ for low-viability cells, and the highest degradation percentage of 60% was gained with highest chlorine dose of 8 mg L^{-1} whilst only 7% of total toxin was degraded with chlorine of 1 mg L^{-1} (Fig. 6b).

To compare total toxin degradation of high- and low-viability

Microcystis after chlorination, modified Chick/Watson model was employed to estimate rate constants (k_{total}) of total toxin degradation over chlorine exposure (Fig. S4) (Daly et al., 2007; Zamyadi et al., 2012b). The fitted equation was shown (Equation (5)):

$$\ln\left(\frac{MC_t}{MC_0}\right) = -k_{total}ct \quad (5)$$

Where ct = chlorine exposure; MC_t = concentration of total toxin after a given chlorine exposure; MC_0 = concentration of total toxin at $ct = 0$; and k_{total} = rate constant of total toxin degradation.

Table 3 showed R² were between 0.91 and 0.99 and RSS ($1.63 \times 10^{-5}\text{--}1.7 \times 10^{-3}$) were much less than 0.05, suggesting the model fitted well. With the same initial chlorination, k_{total} of low-viability cells was much lower than that of high-viability cells ($P < 0.05$) (Table 3). Moreover, average k_{loss} ($50 \pm 27 \text{ M}^{-1} \text{ s}^{-1}$) of low-viability cells was also lower than that of high-viability cells ($98 \pm 56 \text{ M}^{-1} \text{ s}^{-1}$) ($P < 0.05$) (Table 3).

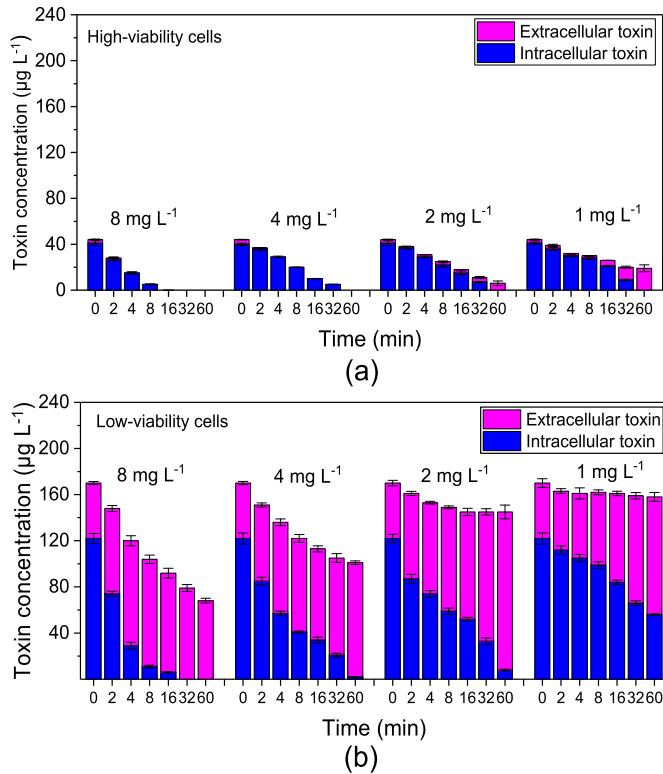


Fig. 6. Intracellular and extracellular toxin of high- (a) and low-viability *Microcystis* (b) treated with various doses of chlorine (1, 2, 4 and 8 mg L⁻¹) after a contact time of 0, 2, 4, 8, 16, 32 and 60 min.

3.5. Intracellular toxin release and extracellular toxin degradation

Both intracellular and extracellular toxin of low-viability cells were higher than that of high-viability cells before chlorination ($P < 0.05$) (Fig. 6). Above results revealed chlorine induced membrane damage of both high- and low-viability *Microcystis* (Fig. 5), and thus, about 50–100% of intracellular toxin was released during chlorination within a contact time of 60 min (Fig. 6). Meanwhile, the released toxin after membrane damage and initial extracellular toxin were degraded via chlorination (Fig. 6). During chlorination for high-viability cells, extracellular toxin was degraded to below detection limits after 4 min with dosages of 4 and 8 mg L⁻¹, but it increased from initial 3 μg L⁻¹ to 6 and 19 μg L⁻¹ with dosages of 2 and 1 mg L⁻¹, respectively (Fig. 6a). In contrast, with chlorination of 1–8 mg L⁻¹ for low-viability cells, extracellular toxin remained at high-level during chlorination and increased from 48 μg L⁻¹ to 68–102 μg L⁻¹ after a contact time of 60 min (the corresponding increase percentage of 42–113%) (Fig. 6b).

To further compare the process of intracellular toxin release and

extracellular toxin degradation with chlorination for high- and low-viability cells, relationship between chlorine exposure, toxin release and degradation can be described as a first-order process and the process can be considered as consecutive reaction, as shown in equation (6). Besides, concentration of intracellular (A) and extracellular toxin (B) are described by equations (7) and (8) (Jones, 1970; Zamyadi et al., 2013; Fan et al., 2014).



$$A = A_0 e^{-k_i ct} \quad (7)$$

$$B = B_0 e^{-k_e ct} + A_0 \left(e^{-k_e ct} - e^{-k_i ct} \right) / (1 - k_e / k_i) \quad (8)$$

Where ct = chlorine exposure; A_0 = concentration of intracellular toxin at $t = 0$ min; A = concentration of intracellular toxin at a given ct value; B_0 = concentration of extracellular toxin at $t = 0$ min; B = concentration of extracellular toxin at a given ct value; k_i = rate constant of intracellular toxin release; k_e = rate constant of extracellular toxin degradation; C = concentration of degraded toxin at a given ct value.

Table 4 showed Nash-Sutcliffe efficiency coefficient (NSE) was ranged of 0.72–0.99, demonstrating the model fitted well. With the same initial dosages of chlorination, k_i of low-viability cells (90–127 M⁻¹ s⁻¹) was higher than high-viability cells (28–102 M⁻¹ s⁻¹), but k_e (18–36 M⁻¹ s⁻¹) was much lower than that of high-viability cells (33–113 M⁻¹ s⁻¹) ($P < 0.05$) (Table 4). Besides, with the same treatment, k_e of high-viability cells was higher than its k_i ($k_e > k_i$) ($P < 0.05$), but contrary result was gained for low-viability cells ($k_e < k_i$) (Table 4). Average values of k_e and k_i also showed the same pattern for both high- and low-viability cells (Table 4).

4. Discussion

4.1. Chlorine decay

During chlorination for both high- and low-viability *Microcystis*, chlorine decay was fast in all treatments, as the same pattern observed by previous studies (Ho et al., 2006; Daly et al., 2007; Zamyadi et al., 2012b, 2013). However, this study found chlorine decay was faster for low-viability cells than high-viability cells with the same initial chlorine dosage (Fig. 4; Table 1). Previous studies have noted that presence of natural organic matters (NOMs) is the most important factor in chlorine consumption, and its concentration and characteristics are known to strongly influence the chlorine reaction, since NOMs contain a higher proportion of conjugated and substituted aromatic moieties is more susceptible to chlorine attack (Reckhow et al., 1990; Korshin et al., 1997; Ho et al., 2006; Deborde and von Gunten, 2008). In this study, we did not use natural waters as backgrounds to conduct chlorination

Table 3

Total toxin degradation rate (k_{total}) of high- and low-viability *Microcystis* treated with various doses of chlorine (1, 2, 4 and 8 mg L⁻¹).

Dose (mg L ⁻¹)	High-viability cells				Low-viability cells			
	k_{total} (M ⁻¹ s ⁻¹)	SE	R ²	RSS	k_{total} (M ⁻¹ s ⁻¹)	SE	R ²	RSS
1	180 ^a	12	0.94	8.88×10^{-3}	89 ^a	5	0.99	7.16×10^{-6}
2	89	6	0.95	6.84×10^{-3}	41 ^a	2	0.99	1.63×10^{-5}
4	56	4	0.91	6.23×10^{-3}	45	3	0.93	4.63×10^{-3}
8	67	2	0.99	1.70×10^{-3}	25	1	0.97	5.27×10^{-3}
Average	98 ± 56				50 ± 27			

SE: standard errors of k_{total} . R²: correlation coefficients. RSS: residual sum of squares.

^a Values were not accurately estimated due to insufficient data.

Table 4
Rate constants of intracellular toxin release (k_i) and extracellular toxin degradation (k_e) of high- and low-viability *Microcystis* treated with various doses of chlorine (1, 2, 4 and 8 mg L⁻¹).

Dose (mg L ⁻¹)	High-viability cells						Low-viability cells					
	k_i (M ⁻¹ s ⁻¹)	SE	NSE	k_e (M ⁻¹ s ⁻¹)	SE	NSE	k_i (M ⁻¹ s ⁻¹)	SE	NSE	k_e (M ⁻¹ s ⁻¹)	SE	NSE
1	102 ^a	9	0.99	105 ^a	13	0.96	118 ^a	15	0.92	27 ^a	5	0.83
2	99	8	0.90	113	7	0.99	106 ^a	8	0.84	23 ^a	2	0.72
4	45	4	0.97	52	2	0.81	127	9	0.95	36	4	0.99
8	28	2	0.98	33	3	0.90	90	8	0.91	18	1	0.97
Average	69 ± 38			76 ± 39			110 ± 16			26 ± 8		

SE: standard errors of k_i and k_e . NSE: Nash-Sutcliffe efficiency coefficient.

^a Values were not estimated accurately due to insufficient data.

experiments, as done by previous studies (Ho et al., 2006; Daly et al., 2007; Lin et al., 2009; Zamyadi et al., 2012b; Fan et al., 2016). Nonetheless, these samples of high- and low-viability cells collected from cultures in BG-11 medium (no organic matters) could better show the influence of the change of cell viability on water quality backgrounds, because cyanobacteria could secrete extracellular organic matters (EOMs) to cultures during growth and some studies found characteristics of EOMs were changing at different growth phase and DOC increased from exponential to stationary phase (Henderson et al., 2008; Pivokonsky et al., 2014). Further analysis of EOMs in our samples showed low-viability cells exhibited higher extracellular DOC and UV₂₅₄ than high-viability cells ($P < 0.05$) (Table 5). UV₂₅₄ representing the aromatic character has been identified as a potential surrogate measure for DOC (Korshin et al., 2009), suggesting higher concentration of EOMs accumulated in low-viability cells, as well as more aromatic groups in EOMs. Thus, chlorine consumption for low-viability cells was much faster than for high-viability cells with the same initial dosages of chlorination. SUVA could describe the nature of NOMs in the water in terms of hydrophobicity and hydrophilicity, and a SUVA < 3 illustrates mainly hydrophilic material (Edzwald and Tobiason, 1999). Here, a value of 1.67 and 1.75 L mg⁻¹ m⁻¹ were measured for high- and low-viability cells, respectively (Table 5), suggesting EOMs of these samples mainly contained hydrophilic organic matters. However, there was no significant difference of SUVA between high- and low-viability cells ($P > 0.05$) (Table 5), demonstrating difference in chlorine decay was not correlated with the hydrophilicity of EOMs.

4.2. Membrane integrity loss

Chlorination of 1–8 mg L⁻¹ could completely destroy membrane integrity of high-viability cells (Fig. 5a), in agreement with previous studies (Daly et al., 2007; Zamyadi et al., 2010, 2012b; 2013; Fan et al., 2013). Fan et al. (2013) found chlorine was the most efficient oxidant to destroy membrane of cyanobacteria at exponential phase, compared to other oxidants (e.g., KMnO₄, H₂O₂). Here, with the same initial chlorine dosage, chlorine exposure for low-viability cells was a lower level than for high-viability cells (Fig. 4), but

Table 5
A comparison of DOC, UV₂₅₄ and SUVA of samples of high- and low-viability *Microcystis* prior to chlorination.

Parameters	DOC (mg L ⁻¹)		UV ₂₅₄ (cm ⁻¹)		SUVA (L mg ⁻¹ m ⁻¹)	
	Mean	SD	Mean	SD	Mean	SD
High-viability cells	5.1	0.2	0.085	0.01	1.67	0.04
Low-viability cells	12.4	0.4	0.217	0.05	1.75	0.03

Mean: mean value of three parallel samples.

SD: standard deviation values.

complete loss of membrane integrity of low-viability cells was observed in all treatments. These results suggested chlorination had strong capacity to inactivate both high- and low-viability cells via completely destroy membrane integrity.

Besides, for low-viability cells, the membrane damage rate (k_{loss}) was higher than high-viability cells (Table 2). Fan et al. (2016) and He and Wert, 2016 found colonial *Microcystis* was more resistant to chlorination than unicellular *Microcystis*, since colonies can be protected by surface amorphous mucilage or sheaths. These results suggested cellular surface structures are important barriers for protection from chlorine attack. Comparing with high-viability cells, both TEM and SEM showed cellular surface structures (e.g., sheath) of low-viability cells were destroyed to some extent, resulting in incapacity to maintain its spherical shape (Fig. 2e and f). Consequently, low-viability *Microcystis* was less resistant to chlorination, leading to higher membrane damage rate (k_{loss}) than high-viability cells.

4.3. Total toxin degradation

Total toxin was degraded to some extent (7–100%) after chlorination for both high- and low-viability *Microcystis* depending on chlorine exposure (Fig. 6), as demonstrated by previous studies that chlorination was efficient to oxidize cyanotoxins under various water quality backgrounds (Nicholson et al., 1994; Acero et al., 2005, 2008; Ho et al., 2006; Merel et al., 2010; Zamyadi et al., 2010, 2012b; 2013; Fan et al., 2014, 2016). For high-viability cells, chlorination could oxidize total toxin to below detection limits with ct value of >30 mg min L⁻¹, while 6 and 19 µg L⁻¹ of total toxin were present after 60 min with ct value of 1.6–9.6 mg min L⁻¹ (Fig. 4a; 6a). It suggested sufficient chlorine exposure was important for complete toxin oxidation, and Nicholson et al. (1994) also firstly noted that cyanotoxins were completely destroyed under conditions that a chlorine residual of at least 0.5 mg L⁻¹ was present after a contact time of 30 min. However, when low-viability cells were treated with sufficient chlorine exposure of as high as 36 mg min L⁻¹, 68 µg L⁻¹ of total toxin was also present after 60 min even with chlorine residual of 0.6 mg L⁻¹ (Fig. 4b; 6b). These results indicated incomplete toxin oxidation for low-viability cells was not only due to insufficient chlorine exposure.

Actually, rate constants of total toxin degradation for low-viability cells was much lower than high-viability cells (Table 3), implying incomplete toxin oxidation for low-viability cells with sufficient chlorine exposure would attribute to the decrease of k_{total} . Literatures concluded that chlorination conditions (e.g., temperature, pH, water matrix) would strongly affect cyanotoxin degradation (Nicholson et al., 1994; Acero et al., 2005). In this study, chlorination experiments were conducted at the same temperature and pH, but initial concentration of total toxin and reaction backgrounds showed the difference between high- and low-viability cells (Fig. 6). It is possible that the much higher initial

concentration of total toxin in low-viability cells ($170 \mu\text{g L}^{-1}$) than high-viability cells ($44 \mu\text{g L}^{-1}$) would lead to incomplete degradation of total toxin with sufficient chlorine exposure. However, Nicholson et al. (1994) and Acero et al. (2005) reported much higher concentration of MC-LR ($200\text{--}300 \mu\text{g L}^{-1}$) could be completely degraded with low chlorine exposure ($1\text{--}2 \text{mg L}^{-1}$ for less than 30 min). Thus, it was not the main factor to affect total toxin degradation by chlorination for low-viability cells.

Effect of higher initial concentration of DOC of low-viability cells on chlorine consumption and toxin oxidation could not be ignored in this study. He and Wert, 2016 have tried to employ the ratio of chlorine dosages to initial DOC [chlorine: DOC] to minimize the effect of initial DOC on chlorination to treat cyanobacteria. Hence, we further re-evaluated values of [chlorine: DOC] in various treatments and found that the k_{total} ($25 \pm 1 \text{M}^{-1} \text{s}^{-1}$) of low-viability cells was still lower in the treatment with higher value of [chlorine: DOC = 0.65] than high-viability cells with lower value of [chlorine: DOC = 0.39] ($89 \pm 6 \text{M}^{-1} \text{s}^{-1}$) (Table S1). These results suggested higher initial concentration of DOC could affect chlorine decay, but it was not the main factor to decrease k_{total} of low-viability cells.

Chlorine could undergo reactions with numerous organic compounds and second-order rate constants for chlorination vary over 10 orders of magnitude (i.e. $0.1\text{--}109 \text{M}^{-1} \text{s}^{-1}$) depending on particular sites of organic compounds (Deborde and von Gunten, 2008). Besides, in various water matrix, cyanotoxin degradation rate by chlorine was estimated by many studies and varied from 22 to $241 \text{M}^{-1} \text{s}^{-1}$ (Table S2). Daly et al. (2007) and Ho et al. (2006) reported rate constants was higher in natural waters than ddH_2O , and Ho et al. (2006) attributed the differences to NOMs-microcystin interactions. In this study, decrease of k_{total} for low-viability cells might be also attributed to EOMs-cyanotoxin interactions. Ziegmann et al. (2010) found the highest fluorescence intensity of protein-like substances in EOMs at decline phase. Besides, *M. aeruginosa* could produce many other cyclic peptides similar to microcystin and some of these peptides had greater reactivity with chlorine than cyanotoxin molecules (Hureiki et al., 1994; Ho et al., 2006). It suggested that there may be more peptides similar to microcystin present in low-viability cells, which could inhibit cyanotoxin degradation via competitive reactions. Nonetheless, chlorine reaction with cyanotoxins is a complex interaction with organic matters, and characteristics of EOMs in low-viability cells was not well investigated in this study. Therefore, more studies were required to elucidate EOMs-cyanotoxin interactions.

4.4. Intracellular toxin release and extracellular toxin degradation

Chlorination could completely destroy membrane integrity for both high- and low-viability cells, and thus, the release of intracellular toxin could not be avoided when chlorine was applied to treat cyanobacteria in practice. Above study has demonstrated low-viability cells was less resistant to chlorination than high-viability cells (Table 2), indicating its membrane damage would be more serious than high-viability cells after chlorination. Hence, its rate constants of intracellular toxin release were higher than high-viability cells, in line with membrane damage rate constants (k_{loss} , low-viability > high-viability) (Table 2; 4). Meanwhile, for low-viability cells, rate constants of extracellular toxin degradation strikingly declined compared to high-viability cells (Table 4). It might also result from EOMs-cyanotoxin interactions, as the same as k_{total} .

For high-viability cells, there was no increase of extracellular toxin during chlorination with initial dose of 4 and 8mg L^{-1} (Fig. 6a). The same results were also observed by Zamyadi et al. (2013) and Fan et al. (2014), attributed to the higher rate of extracellular toxin degradation (k_e) than intracellular toxin release (k_i)

($k_e > k_i$). In this study, k_e was also higher than k_i (Table 4). However, an increase of extracellular toxin occurred with ct value of $1.6\text{--}9.6 \text{mg min L}^{-1}$, since the released extracellular toxin could not be effectively degraded after 16–32 min without chlorine residual (Fig. 6a). In contrast, with sufficient chlorine exposure of $>30 \text{mg min L}^{-1}$, extracellular toxin kept decreasing and it was degraded to below the safety guideline of $1 \mu\text{g L}^{-1}$ for drinking water by WHO (Fig. 6a), suggesting both $k_e > k_i$ and sufficient chlorine exposure were important for the control of extracellular toxin risk when chlorination was applied to treat high-viability cells.

For low-viability cells, insufficient chlorine exposure of $0.6\text{--}9.6 \text{mg min L}^{-1}$ could cause an increase of extracellular toxin after chlorination, as the same for high-viability cells. However, even with sufficient chlorination exposure of 36mg min L^{-1} , extracellular toxin remained increasing during chlorination as well (Fig. 4b; 6), suggesting the rapid released toxin could not be effectively degraded due to the decrease of k_e for low-viability cells (Fig. 6b; Table 4). Meanwhile, k_i of low-viability cells was much higher than high-viability cells. Hence, for low-viability cells, continuous increase of extracellular toxin was mainly attributed to its much higher k_i than k_e ($k_e < k_i$). Of note, initial concentration of extracellular ($48 \mu\text{g L}^{-1}$) in low-viability cells was much higher than high-viability cells ($3 \mu\text{g L}^{-1}$) (Fig. 6), and thus, there was much higher concentration of extracellular toxin of $68\text{--}137 \mu\text{g L}^{-1}$ present after 60 min with chlorination for low-viability cells. Consequently, chlorination for low-viability cells would pose a high risk of extracellular toxin.

4.5. Practical implications

This study concluded that chlorination could be employed as an oxidant to treat high-viability cyanobacteria and prevent the breakthrough of extracellular toxin into drinking water, in agreement with previous studies (Zamyadi et al., 2013; Fan et al., 2014, 2016). Nonetheless, chlorination may not be a feasible option to treat low-viability cyanobacteria at decline stage of cyanobacterial blooms. These results suggested chlorination application to treat algal-laden source waters would be limited by the stage of a successive cyanobacterial bloom. Therefore, monitoring of cell-viability of cyanobacteria may be necessary for water suppliers to manage drinking water quality during a successive bloom. Optimizing chlorination or further evaluating other water treatment processes to treat low-viability cyanobacteria would be an important issue in the further work.

5. Conclusions

This study was the first report to show that the change of cell-viability of cyanobacteria could challenge chlorination to treat algal-laden source waters during a successive bloom. Some of the key findings were shown below:

- (i) Chlorine exposure was lower for low-viability cells than high-viability cells with the same initial dosage of chlorine, mainly due to faster chlorine consumption resulting from its rise of DOC and more aromatic groups in EOMs.
- (ii) Low-viability cells were less resistant to chlorine oxidation than high-viability cells, leading to higher rate of membrane damage (k_{loss}) and intracellular toxin release (k_i).
- (iii) Total/extracellular toxin degradation efficiency (k_{total}/k_e) of chlorination for low-viability cells strikingly declined and it may be attributed to EOMs-cyanotoxin interactions.
- (iv) Total toxin could be completely oxidized for high-viability cells with sufficient chlorine exposure ($>30 \text{mg min L}^{-1}$)

but chlorination could not work well for low-viability cells even with chlorine exposure of as high as 36 mg min L⁻¹.

- (v) Extracellular toxin of high-viability cells remained decreasing with sufficient chlorine exposure due to $k_e > k_i$ whereas a continuous increase occurred for low-viability cells due to the changed pattern of $k_e < k_i$.

Declaration of competing interest

The authors declare that they have no known competing financial interests or personal relationships that could have appeared to influence the work reported in this paper.

Acknowledgements

This work was supported by National Key R&D Program of China (2017YFE0107300), Science and Technology Project of Water Resources Department of Fujian Province (MSK201711), Science and Technology Major Project of Xiamen (3502Z20171003) and K.C.Wong Education Foundation. Special thanks were also addressed to our partner Dr. Jiajia Fan to help us revise draft-manuscript.

Appendix A. Supplementary data

Supplementary data to this article can be found online at <https://doi.org/10.1016/j.watres.2020.115769>.

References

- Acero, J.L., Rodriguez, E., Meriluoto, J., 2005. Kinetics of reactions between chlorine and the cyanobacterial toxins microcystins. *Water Res.* 39 (8), 1628–1638.
- APHA, AWWA, WEF, 1998. Standard Methods for the Examination of Water and Wastewater, twentieth ed. American Public Health Association, American Water Works Association, and Water Environment Federation, Washington, DC, USA.
- Daly, R.I., Ho, L., Brookes, J.D., 2007. Effect of chlorination on *Microcystis aeruginosa* cell integrity and subsequent microcystin release and degradation. *Environ. Sci. Technol.* 41, 4447–4453.
- Deborde, M., von Gunten, U., 2008. Reactions of chlorine with inorganic and organic compounds during water treatment—kinetics and mechanisms: a critical review. *Water Res.* 42 (1–2), 13–51.
- Edzwald, J.K., Tobiason, J.E., 1999. Enhanced coagulation: USA requirements and a broader view. *Water Sci. Technol.* 40 (9), 63–70.
- Falconer, I.R., Beresford, A.M., Runnegar, M.T., 1983. Evidence of liver damage by toxin from a bloom of the blue-green alga, *Microcystis aeruginosa*. *Med. J. Aust.* 1 (11), 511–514.
- Fan, J.J., Ho, L., Brookes, J.D., 2013. Evaluating the effectiveness of copper sulphate, chlorine, potassium permanganate, hydrogen peroxide and ozone on cyanobacterial cell integrity. *Water Res.* 47, 5153–5164.
- Fan, J.J., Hobson, P., Brookes, J.D., 2014. The effects of various control and water treatment processes on the membrane integrity and toxin fate of cyanobacteria. *J. Hazard Mater.* 264, 313–322.
- Fan, J., Rao, L., Lin, T.F., 2016. Impact of chlorine on the cell integrity and toxin release and degradation of colonial *Microcystis*. *Water Res.* 102, 394–404.
- Guo, L., 2007. ECOLOGY: doing battle with the green monster of Taihu Lake. *Science* 317 (5842), 1166–1166.
- Harke, M.J., Steffen, M.M., Paerl, H.W., 2016. A review of the global ecology, genomics, and biogeography of the toxic cyanobacterium, *Microcystis* spp. *Harmful Algae* 54, 4–20.
- He, X., Wert, E.C., 2016. Colonial cell disaggregation and intracellular microcystin release following chlorination of naturally occurring *Microcystis*. *Water Res.* 101, 10–16.
- He, X., Liu, Y.L., Walker, H.W., 2016. Toxic cyanobacteria and drinking water: impacts, detection, and treatment. *Harmful Algae* 54, 174–193.
- Henderson, R.K., Baker, A., Jefferson, B., 2008. Characterization of algogenic organic matter extracted from cyanobacteria, green algae and diatoms. *Water Res.* 42 (13), 3435–3445.
- Ho, L., Onstad, G., Newcombe, G., 2006. Differences in the chlorine reactivity of four microcystin analogues. *Water Res.* 40 (6), 1200–1209.
- Hureiki, L., Croue, J.P., Legube, B., 1994. Chlorination studies of free and combined amino acids. *Water Res.* 28, 2521–2544.
- Jones, C.T., 1970. Determination of the kinetic constants of two consecutive first order reactions. *Biochem. J.* 118 (5), 810–812.
- Kasich, J.R., Taylor, M., Butler, C.W., 2014. Public Water System Harmful Algal Bloom Response Strategy. Ohio Environmental Protection Agency.
- Korshin, G.V., Li, C.W., Benjamin, M.M., 1997. Monitoring the properties of natural organic matter through UV spectroscopy: a consistent theory. *Water Res.* 31 (7), 1787–1795.
- Korshin, G., Chow, C.W.K., Drikas, M., 2009. Absorbance spectroscopy based examination of effects of coagulation on the reactivity of fractions of natural organic matter with varying apparent molecular weights. *Water Res.* 43, 1541–1548.
- Li, X., Zeng, X., Shao, Z.Z., 2019. Dissimilatory iron [Fe(III)] reduction and magnetite formation by a novel fermentative, piezophilic bacterium *Anoxybacter fermentans* DY22613^T isolated from East Pacific Rise hydrothermal sediments. *Geomicrobiol. J.* 1–12.
- Lin, T.F., Chang, D.W., Wang, Y.S., 2009. Effect of chlorination on the cell integrity of two noxious cyanobacteria and their releases of odorants. *J. Water Supply Res. Technol. - Aqua* 58 (8), 539–551.
- Maxwell, K., Johnson, G.N., 2000. Chlorophyll fluorescence—a practical guide. *J. Exp. Bot.* 51 (345), 659–668.
- Merel, S., Clément, M., Thomas, O., 2010. State of the art on cyanotoxins in water and their behaviour towards chlorine. *Toxicol.* 55 (4), 677–691.
- Mouchet, P., Bonnelly, V., 1998. Solving algae problems: French expertise and world wide applications. *Water Supply: Res. Technol. AQUA* 47 (3), 125–141.
- Nicholson, B.C., Rositano, J., Burch, M.D., 1994. Destruction of cyanobacterial peptide hepatotoxins by chlorine and chloramine. *Water Res.* 28, 1297–1303.
- Ou, H., Gao, N., Dong, L., 2011. Mechanistic studies of *Microcystis aeruginosa* inactivation and degradation by UV-C irradiation and chlorination with polysynchronous analyses. *Desalination* 272 (1), 107–119.
- Pearson, L., Mihali, T., Neilan, B., 2010. On the chemistry, toxicology and genetics of the cyanobacterial toxins, microcystin, nodularin, saxitoxin and cylindrospermopsin. *Mar. Drugs* 8 (5), 1650–1680.
- Pietsch, J., Bornmann, K., Schmidt, W., 2002. Relevance of intra- and extracellular cyanotoxins for drinking water treatment. *Acta Hydrochim. Hydrobiol.* 30 (1), 7–15.
- Pivokonsky, M., Safarikova, J., Kopecka, I., 2014. A comparison of the character of algal extracellular versus cellular organic matter produced by cyanobacterium, diatom and green alga. *Water Res.* 51, 37–46.
- Plummer, J.D., Edzwald, J.K., 2002. Effects of chlorine and ozone on algal cell properties and removal of algae by coagulation. *J. Water Supply Res. Technol. - Aqua* 51, 307–318.
- Qi, J., Lan, H., Qu, J., 2016. Pre-chlorination of algae-laden water: the effects of transportation time on cell integrity, algal organic matter release, and chlorinated disinfection byproduct formation. *Water Res.* 102, 221–228.
- Reckhow, D.A., Singer, P.C., Malcolm, R.L., 1990. Chlorination of humic materials: byproduct formation and chemical interpretations. *Environ. Sci. Technol.* 24 (11), 1655–1664.
- Rivasseau, C., Martins, S., Hennion, M.C., 1998. Determination of some physico-chemical parameters of microcystins (cyanobacterial toxins) and trace level analysis in environmental samples using liquid chromatography. *J. Chromatogr. A* 799, 155–169.
- Rodriguez, E., Onstad, G.D., Gunten, U., 2007. Oxidative elimination of cyanotoxins: comparison of ozone, chlorine, chlorine dioxide and permanganate. *Water Res.* 41 (15), 3381–3393.
- Sivonen, K., Jones, G., 1999. Cyanobacterial toxins. In: Chorus, I., Bartram, J. (Eds.), *Toxic Cyanobacteria in Water: a Guide to Their Public Health Consequences, Monitoring and Management*. E & FN Spon, London, UK, pp. 41–111.
- Tang, M.X., Krausfeldt, L.E., Wilhelm, S.W., 2018. Seasonal gene expression and the ecophysiological implications of toxic *Microcystis aeruginosa* blooms in Lake Taihu. *Environ. Sci. Technol.* 52 (19), 11049–11059.
- Watson, S.B., Boyer, G.L., 2013. Harmful and nuisance algae. In: IJC working group (Ed.), *Technical Report on Ecosystem Indicators Assessment of Progress towards Restoring the Great Lakes*. International Joint Commission.
- WHO, 2014. *Guidelines for Drinking Water Quality*, fourth ed., vol. 8. World Health Organization, Geneva.
- Zamyadi, A., Ho, L., Prévost, M., 2010. Release and oxidation of cell-bound saxitoxins during chlorination of *Anabaena circinalis* cells. *Environ. Sci. Technol.* 44 (23), 9055–9061.
- Zamyadi, A., MacLeod, S.L., Prévost, M., 2012a. Toxic cyanobacterial breakthrough and accumulation in a drinking water plant: a monitoring and treatment challenge. *Water Res.* 46, 1511–1523.
- Zamyadi, A., Ho, L., Prévost, M., 2012b. Fate of toxic cyanobacterial cells and disinfection by-products formation after chlorination. *Water Res.* 46 (5), 1524–1535.
- Zamyadi, A., Fan, Y., Prévost, M., 2013. Chlorination of *Microcystis aeruginosa*: toxin release and oxidation, cellular chlorine demand and disinfection by-products formation. *Water Res.* 47 (3), 1080–1090.
- Ziegmann, M., Abert, M., Frimmel, F.H., 2010. Use of fluorescence fingerprints for the estimation of bloom formation and toxin production of *Microcystis aeruginosa*. *Water Res.* 44 (1), 195–204.